



Journal Homepage: - www.journalijar.com

INTERNATIONAL JOURNAL OF ADVANCED RESEARCH (IJAR)

Article DOI: 10.21474/IJAR01/17682

DOI URL: <http://dx.doi.org/10.21474/IJAR01/17682>



RESEARCH ARTICLE

STUDY OF PHYSICAL AND LUMINESCENCE PROPERTIES ND IONS - DOPED Te-W-Pb GLASSES

Rajiv Pandey, A. K. Sharma and Ghizal F. Ansari

Department of Physics, Madhyanchal Professinal University, Ratibad, Bhopal, India.

Manuscript Info

Manuscript History

Received: 05 August 2023

Final Accepted: 09 September 2023

Published: October 2023

Key words:-

X-Ray Diffraction, Differential Scanning Calorimetry, Luminescence

Abstract

New Te-W-Pb oxide base glasses codoped with neodymium oxide have been prepared by traditional melt and quench method. X-ray diffraction (XRD) is done for the confirmation of glassy structure of samples. Differential scanning calorimetry (DSC) gives the information of thermal properties of prepared glasses. Raman spectra are studied to get structural information of glasses. The spectroscopic properties of Nd^{3+} were examined. Infrared emission at 878, 1062, and 1339 nm were seen during stimulation at 804 nm using a diode laser.

Copy Right, IJAR, 2023., All rights reserved.

Introduction:-

Lanthanide (Ln) doped materials have become increasingly important in recent years in the development of low cost integrated laser sources, integrated optical amplifiers, displays, sensors, up-conversion fibres, and low loss components [1]. The research on rare earth doped glasses has been sparked by the aforementioned uses for Lanthanide (Ln) doped materials [2–5]. Neodymium ion is one of the most effective Lanthanide (Ln) ions for creating solid-state lasers due to its high emission at 1060 nm [6]. In order to create high power NIR (at 1060 nm) solid state lasers, trivalent neodymium (Nd^{3+}) ion doped varieties of crystals and glasses were extensively studied under 808 and 885 nm laser diode excitation [7]. For this objective, a variety of glass hosts including the borates, phosphates, germanates, zinc, bismuth and tellurite families have been widely explored [8–11]. The Tellurite-Tungsten- Lead ($\text{TeO}_2\text{-WO}_3\text{-PbO}$) glass system (TWP) stands out among all oxide glasses in terms of its optical characteristics. Tellurite-based glasses can have great mechanical stability, good corrosion resistance, and low phonon energies equal to 750 cm^{-1} in addition to possessing high linear and third order nonlinear optical constants (nonlinear refractive indices). Due to all of these novel characteristics, their transition range has been expanded to the mid-IR (5–6 μm) area. Glasses made of tellurite also have a good capability for absorbing lanthanide dopants in a range of concentrations [12]. Tellurite glasses' high refractive index, prolonged transmission range, and low phonon energy enable the detection of laser emission from rare earth ions over a broad spectral range [13–15]. Optical waveguides can benefit from the use of such materials. A precise noble semi-conducting transition-metal oxide that has captured significant interest for a number of years is tungsten oxide (WO_3). It is also one of the materials that is studied and used the most for electro-chromic and photo-chromic devices, where coloration and bleaching may be obtained through an electro-chemical method [16] and has numerous uses in sensors, display systems, and smart windows. Due to the fact that Ln ions can exist in multiple valence states, i.e., W^{6+} , W^{5+} , and W^{4+} regardless of their initial oxidation state in glasses, tungsten ions are also capable of influencing the luminescence properties of Ln ions in tellurite glasses [17–21]. Therefore, by adding WO_3 at various concentrations, the environment around the doped rare earth ions in the tellurite glass network may be altered efficiently. As a result, intriguing modifications to the luminescence properties of lasing ions are anticipated. Lead-based (PbO) glasses are thought to be of particular relevance at the moment due to their successful application in IR fibre optics, laser windows, and multi-functional

Corresponding Author:- Rajiv Pandey

Address:- Department of Physics, Madhyanchal Professinal University, Ratibad, Bhopal, India.

optical elements. These glasses are more robust against ambient moisture and highly transparent in the mid-infrared range up to 8 μm . In the realm of solid state batteries as power sources, they are also thought to be more advantageous materials for electrochemical applications [22]. Both lead oxide (PbO) and lead fluoride (PbF_2) are effective glass modifiers [23–24]. When added to tungsten tellurite glass, lead oxide (PbO), in particular with its lower phonon energies (346 cm^{-1}), can significantly lower the phonon energies of the host glass and ultimately enhance their radiative transition rates. It is good knowledge that a glass substrate with lower phonon energy greatly promotes radiative transition rates and is extremely beneficial for the design and advancement of photonic devices. In the current study, we created a system called Lead Tungsten Tellurite (TWP) glass using the aforementioned chemicals as constituent elements and doped it with Nd^{3+} ions at various concentrations to study their spectral response, NIR emission, and decay spectral characteristics in order to investigate the potential use of these novel materials for photonic devices in the future.

Glass Preparation

The TWP glasses were created using the melt quenching method using high purity chemicals (more than 99.7%) in 15 g quantities. The TWP glasses had the following composition (in mol%): $(70-x)\% \text{TeO}_2 + 15\% \text{PbO} + 15\% \text{WO}_3 + x\% \text{Nd}_2\text{O}_3$ (here $x = 0, 0.5$ and 1.0 mol%). Based on the Nd^{3+} ion concentration, these glasses are designated as TWP0, TWPNd1, and TWPNd2, respectively. To obtain a smooth powder, batches having various concentrations of Nd^{3+} ions in base glass compositions were thoroughly combined in an agate mortar. These powders were then gathered in a silica crucible and cooked for 30 minutes at 730°C in a furnace. The melt was swiftly pushed by another plate after being quickly poured onto a copper plate with a circular form. To alleviate thermal stresses and increase the mechanical strength of the manufactured TWPNd glasses, they were annealed at 400°C for two hours. In order to prepare the glasses for experiment results, they were lastly polished using emery paper.

Results and Discussion:-

XRD

Since oxide-containing glasses make the process of micro-/nanocrystals precipitation for the production of glass-ceramics quite simple, one must be cautious when manufacturing amorphous materials to ensure that the phenomena do not occur. XRD diffractograms were gathered, as shown in Fig. 1, to ascertain the amorphous structure of the glasses by ruling out significant crystallization. In line with expectations, only very broad amorphous bands [25] rather than sharp peaks are visible in the XRD patterns. Therefore, it can be assumed that no crystallization, or at least none of a magnitude detectable by X-Ray diffraction, occurred during melt solidification.

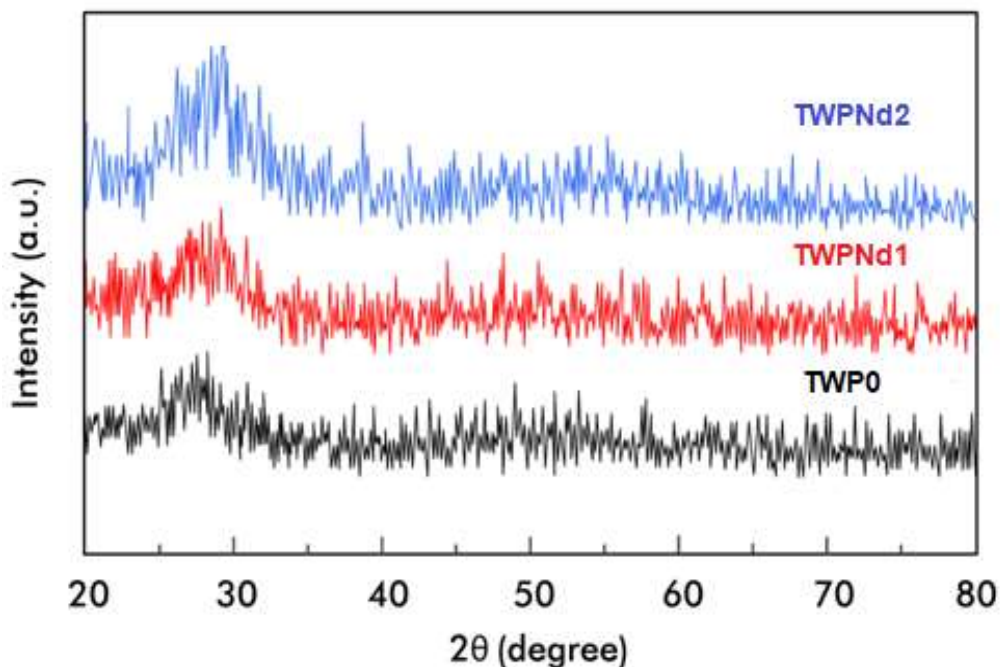


Fig.1:- XRD plot of $\text{TeO}_2[70-x]-\text{WO}_3[15]-\text{PbO}[15]-[x]\text{Nd}_2\text{O}_3$ samples.

Differential Scanning calorimetry (DSC)

Fig. 2 shows DSC curves obtained for the all glass samples. The characteristic temperatures (Glass transition (T_g), crystallization onset (T_x) and crystallization maximum (T_p) temperatures). The value of T_g , and T_x for undoped glass sample could be observed at $T_g = 360$ °C, and $T_x = 486$ °C Thermal stability of the glass was evaluated with the $K_2 = T_x - T_g$ parameter proposed by Hruby [26, 27]. The value so obtained of 126 °C, is in agreement with literature [27, 28]. All these values are considered high, which means the glass matrix displays high thermal stability against crystallization on heating [28].

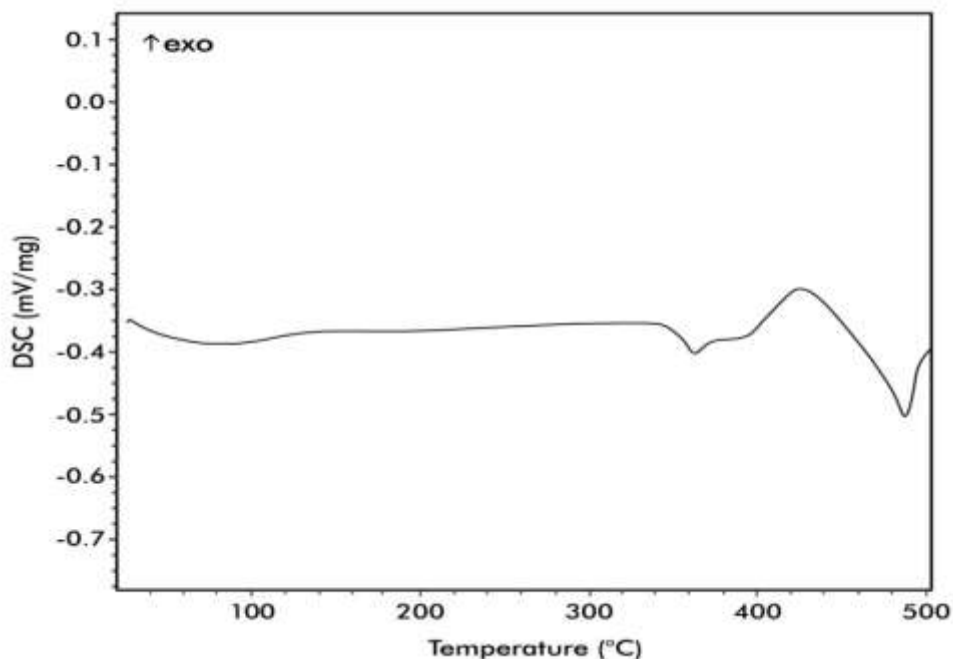


Fig. 2:- Thermogram of TWPND2 sample.

Raman spectra

The Raman spectra of the glass samples, 70% TeO_2 , 15% WO_3 , and 15% PbO , are shown in Fig. 3. Five bands are present in the (TWP0) glass's Raman spectrum at wavenumbers of 930, 858, 730, 479, and 355 cm^{-1} . According to Raman research on tungsten tellurite glasses, the detected band around 930 cm^{-1} is attributed to symmetric stretching vibrations of W-O- and W=O bonds connected to WO_6 units, and the Raman band at 858 cm^{-1} is attributed to stretching vibrations of W-O-W in WO_4 or WO_6 units [29- 31]. The band around 730 cm^{-1} is attributed to symmetric stretching vibrations among Te and non-bridging oxygen (NBO) in TeO_{3+1} units (The TeO_{3+1} unit can be thought of as a distorted trigonal bipyramidal (TeO_4) unit including one oxygen further away from the core tellurium than the other three oxygens) or possibly to the stretching mode of TeO_3 unit [18], most likely to Te=O bond. The band around 730 cm^{-1} is typical stretching vibrations of Te-O-W or Te-O-Te connections are responsible for the 479 cm^{-1} Raman band. The bending vibrations of W-O-W in WO_6 units are thought to be the cause of the band at 355 cm^{-1} , which symbolises the distinctive bonding of tungsten glasses [29–31]. Significant alterations in the Raman spectra resulting from the tellurite network and the tungsten network are brought about by the equimolar replacement of WO_3 by PbO . As seen in Fig. 3, the Raman band shifts and the intensity of the bands at about 479-445 cm^{-1} drops, which suggests that Te-O-W or Te-O-Te links are broken and that some Te-O-Pb linkages are forming at the expense of Te-O-Te or Te-O-W linkages [32-33]. According to Fig.3, the Raman band shifts from 343 to 320 cm^{-1} and the band at 355 cm^{-1} (TWP0) to 343 cm^{-1} (TWP3) as the PbO level rises from 10 to 20 mol%. This is supported by the Raman band's emergence near 320-336 cm^{-1} , which is caused by Pb-O vibration in PbO_4 units [34]. The band at 730 cm^{-1} suffers as the intensity of the shoulder at 658 cm^{-1} increases, however the position of this band (730 cm^{-1}) is unaffected by the PbO content. This suggests that in the current system, PbO up to 20 mol% serves as a network modifier. When PbO is present in small amounts (up to 20 mol%), it enters the glass network by dissolving Te-O-Te and Te-O-W bonds (normally, PbO 's oxygen breaks local symmetry while Pb^{2+} ions occupy interstitial positions) and introducing coordinate defects known as unpaired electrons. These coordinate defects then implement non-bridging oxygen ions, which in turn neutralize the negative charge of non-bridging

oxygen atoms and reduce As a result, the glass network becomes less deformed, which also raises the possibility that WO₄ units may develop at a high PbO levels. This explains why the addition of PbO content causes the band at 858-831 cm⁻¹ and the band at 930-895 cm⁻¹ to shift towards lower wave numbers.

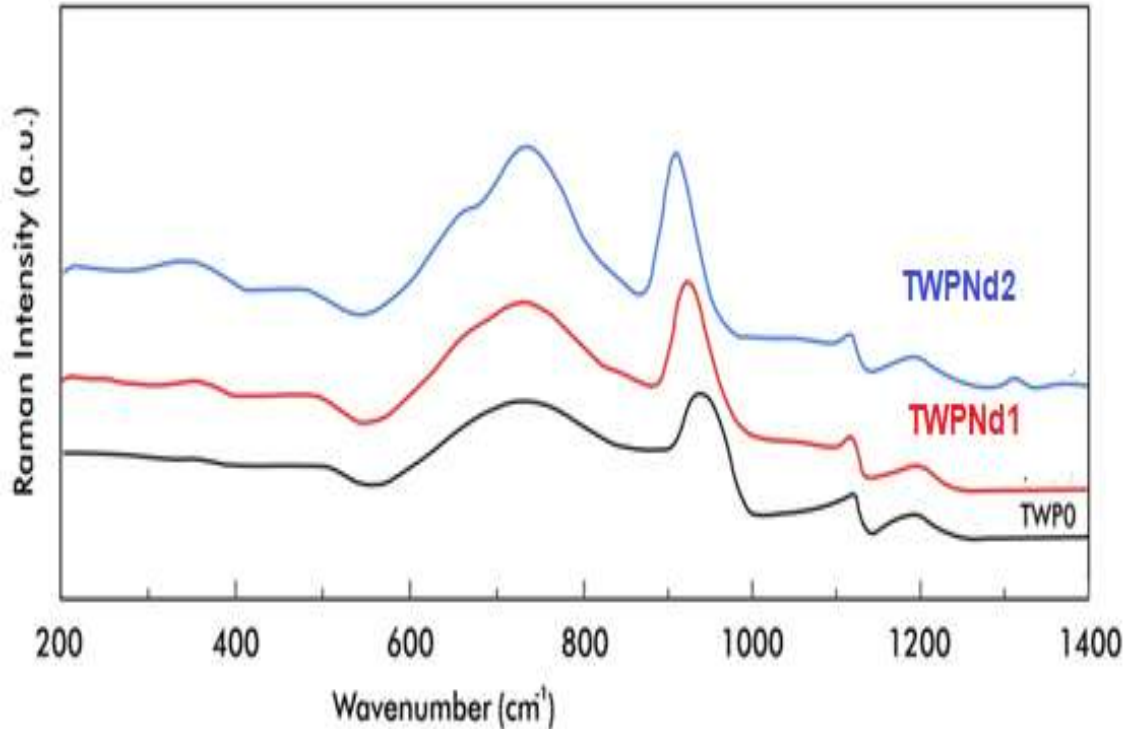


Fig 3:- Raman spectra of TWP0, TWPNd1 and TWPNd2 glasses.

Optical Absorption Spectra

At ambient temperature, optical absorption spectra in the visible and near infrared (VIS-NIR) ranges between 400 and 1000 nm were recorded for all of the TWP glasses doped with Nd³⁺ ions. Each spectrum has similar band locations with a small variation in the strength of the individual absorption bands. The optical absorption spectra of TWP glasses doped with Nd³⁺ ions in the VIS-NIR band are displayed in Fig. 4. All TWP glasses include Nd³⁺ ions, and these ions exhibit eight absorption bands in the VIS-NIR region at 513, 526, 584, 627, 681, 748, 803, and 877 nm [5.37, 5.38], which corresponding to the transitions ${}^4I_{9/2} \rightarrow {}^4G_{9/2}$, ${}^4I_{9/2} \rightarrow {}^4G_{7/2}$, ${}^4I_{9/2} \rightarrow {}^4G_{5/2}$, ${}^4I_{9/2} \rightarrow {}^2H_{11/2}$, ${}^4I_{9/2} \rightarrow {}^4F_{9/2}$, ${}^4I_{9/2} \rightarrow {}^4F_{7/2}$, ${}^4I_{9/2} \rightarrow {}^4F_{5/2}$, and ${}^4I_{9/2} \rightarrow {}^4F_{3/2}$ respectively [39, 40]. Few absorption bands have vanished in the UV region due to the host glass's significant UV absorption.

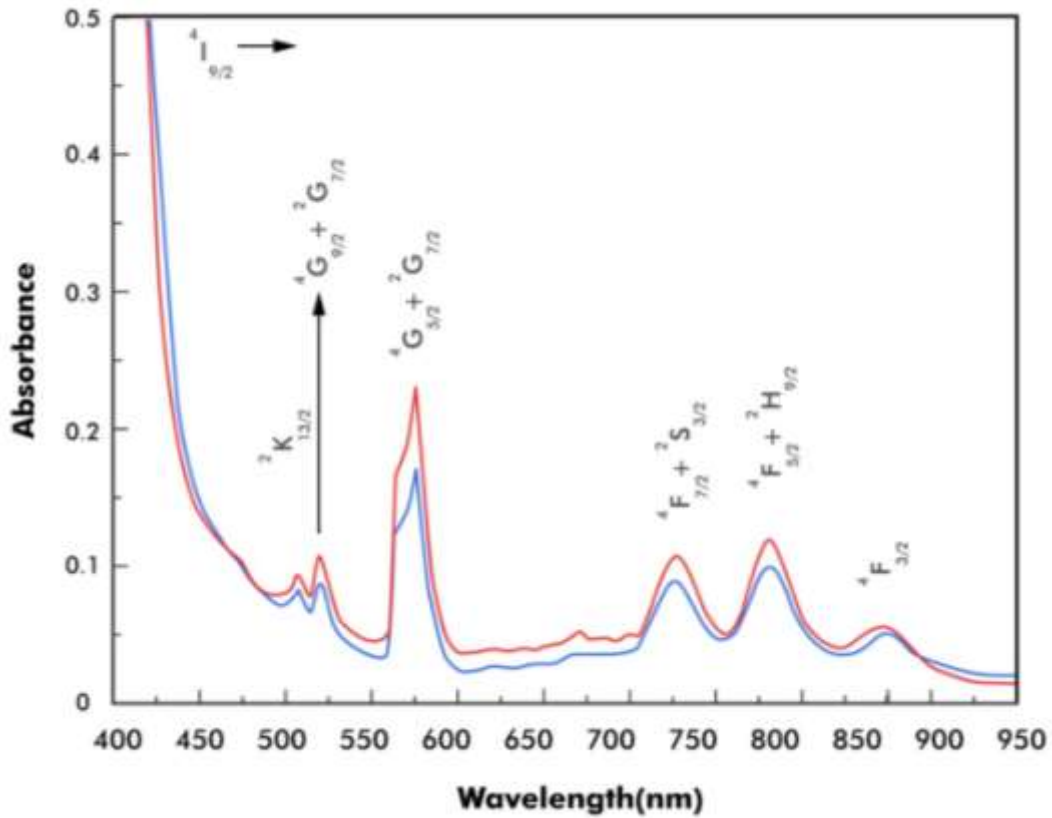


Fig 4:- Absorption spectra of TWPNd1 and TWPNd2 glasses.

Photoluminescence Spectra and Radiative Properties

Fig. 5 displays the NIR photoluminescence spectra of TWP glasses doped with Nd^{3+} ions stimulated by an 808 nm light.

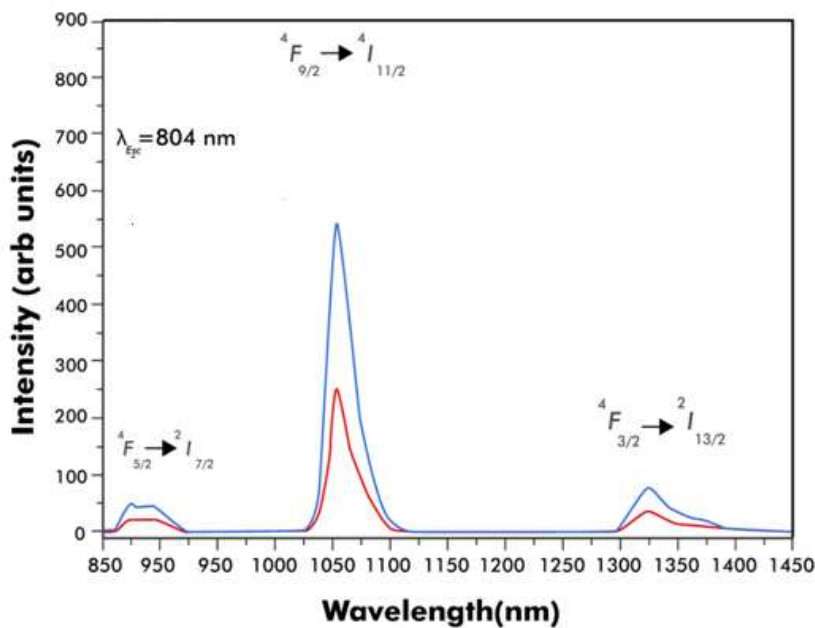


Fig 4, NIR photoluminescence spectra of TWP glasses doped with Nd^{3+} ions stimulated by an 804 nm light.

As shown in Fig. 5, the Nd^{3+} ions stimulated to the ${}^4\text{F}_{5/2}$ level in TWP glasses immediately relax to the ${}^4\text{F}_{3/2}$ metastable state by fast non-radiative relaxation. Three emission bands at 878, 1062, and 1339 nm, which correlate to the transitions ${}^4\text{F}_{3/2} \rightarrow {}^4\text{I}_{9/2}$, ${}^4\text{F}_{3/2} \rightarrow {}^4\text{I}_{11/2}$, and ${}^4\text{F}_{3/2} \rightarrow {}^4\text{I}_{13/2}$, respectively, make up the resulting PL spectra shown in Fig. 3. It can be seen from the PL spectra that as the Nd^{3+} ion concentration rises up to 1.0 mol%, so does the strength of every emission transition. For TWP2 glass, a transition ${}^4\text{F}_{3/2} \rightarrow {}^4\text{I}_{11/2}$ detected at 1062 nm has the highest intensity out of all the emission transitions. Fig. 4 depicts the absorption, excitation, and emission processes as well as a potential cross-relaxation pathway.

Conclusion:-

There were created new Te-W-Pb oxide glasses. TeO_4 , $[\text{TeO}_3]/[\text{TeO}_{3+1}]$, WO_4 , and WO_6 units make up the glass network, according to the Raman spectra of TeO_2 - WO_3 glasses. TeO_4 , $[\text{TeO}_3]/[\text{TeO}_{3+1}]$, WO_4 and WO_6 , and PbO_4 units make up the glass structure, according to the Raman spectra of TeO_2 - WO_3 - PbO glasses. The glass matrix possesses a high thermal stability against crystallisation on heating as evidenced by the measurement of thermal stability parameters from DSC curves such as T_g and T_x . Te-W-Pb connectivities are created when WO_3 is added to PbO glass, which results in a unique stability of the glasses. The glassy matrix did not alter structurally as a result of the neodymium addition. The spectroscopic properties of Nd^{3+} were examined. Infrared emission at 878, 1062, and 1339 nm were seen during stimulation at 804 nm using a diode laser. Te-W-Pb: Nd during laser operation, highlighting the stated neodymium-doped lead-tungsten-tellurite glass as a very interesting choice for optically active elements in addition to its good spectroscopic characteristics.

References:-

1. A.J Kenyon-Progress in Quantum Electronics Volume 26, Issues 4–5, 2002, Pages 225-284.
2. K. Swapna, Sk. Mahamuda, A. Srinivasa Rao, M. Jayasimhadri, T. Sasikala, L. Rama Moorthy, *Ceram. Int.* 39 (2013) 8459–8465.
3. Sk. Mahamuda, K. Swapna, P. Packiyaraj, A. Srinivasa Rao, G. Vijaya Prakash, *J. Lumin.* 153 (2014) 382–392.
4. Sk. Mahamuda, K. Swapna, M. Venkateswarlu, A. Srinivasa Rao, Suman shakya, G. Vijaya Prakash, *J. Lumin.* 154 (2014) 410–424.
5. K. Swapna, Sk. Mahamuda, A. Srinivasa Rao, T. Sasikala, P. Packiyaraj, L. Rama Moorthy, G. Vijaya Prakash, *J. Lumin.* 156 (2014) 80–86.
6. C. Madhukar Reddy, N. Vijaya, B. Deva Prasad Raju, *Acta Part A Mol. Biomol. Spectrosc.* 115 (2013) 297–304.
7. A. Agnesi, P. Dallochio, F. Pirzio, G. Reali, Compact sub-100-fs Nd:silicate laser, *Opt. Commun.* 282 (2009) 2070–2073.
8. S. Bairagi, K.S. Bartwal, S.K. Dhiman, S.K. Mahajan, G.F. Ansari, *Materials Today: Proceedings.* (2022) S2214785322067177. <https://doi.org/10.1016/j.matpr.2022.10.192>.
9. R.P. Kumbhakar, G.F. Ansari, S.K. Dhiman, A.A. Khan, *IOP Conference Series: Materials Science and Engineering* 1258 (1), 012002
10. H. Gebavi, S. Taccheo, R. Balda, J. M. Fernandez, D. Milanese, F. Auzel, *J. Non-Cryst. Solids* 358 (2012) 11497–11500.
11. G. Liao, Q. Chen, J. Xing, H. Gebavi, D. Milanese, M. Fokine, M. Ferraris, *J. Non-Cryst. Solids* 355 (2009) 447–452.
12. R. El-Mallawany, *Tellurite Glasses Hand Book. Physical Properties and Data*, CRC Press, USA, 2002, p. 376.
13. N. G. Boetti, J. Lousteau, A. Chiasera, M. Ferrari, E. Mura, G. C. Scarpignato, S. Abrate, D. Milanese, *J. Lumin.* 132 (2012) 1265–1269.
14. A. Jha, B. Richards, G. Jose, T. Teddy-Fernandez, P. Joshi, X. Jiang, J. Lousteau, *Prog. Mater Sci.* 57 (2012) 1426–1491.
15. S. Shen, M. Naftaly, A. Jha, *Opt. Commun.* 205 (2002) 101–105.
16. D. Barreca, S. Bozza, G. Carta, G. Rossetto, E. Tondello, P. Zanella, *Surf. Sci.* 532 (2003) 439–443.
17. G. Poirier, F.C. Cassanjes, Y. Messaddeq, S.J.L. Ribeiro, *J. Non-Cryst. Solids* 355 (2009) 441–446.
18. C. Lasbrunag, P. Thomas, O. Masson, J.C. Champarnaud-Mesjard, E. Fargin, V. Rodriguez, M. Lahaye, *Opt. Mater.* 31 (2009) 775–780.
19. P. Subbalakshmi, N. Veeraiyah, *J. Non-Cryst. Solids* 298 (2002) 89–98.
20. Y. Gandhi, K.S.V. Sudhakar, M. Nagarjuna, N. Veeraiyah, *J. Alloys Compd.* 485 (2009) 876–886.
21. Y.B. Saddeek, *Philos. Mag.* 89 (2009) 41–54.
22. G. Damarawi, Transport behaviour of PbO - PbF_2 - TeO_2 Glasses, *Phys. Status Solidi A* 177 (2000) 385–392.

23. G. Vijaya Prakash, R. Jagannathan, *Acta*, Part A 55 (1999) 1799–1808.
24. B. Govinda Rao, H.G. Keshava Sundar, K.J. Rao, Investigations of glasses in the system PbO–PbF₂, *J. Chem. Soc. Faraday Trans. I* 80 (1984) 3491–3501.
25. S.D. Ponja, I.P. Parkin, C.J. Carmalt, Synthesis and material characterization of amorphous and crystalline (a-) Al₂O₃: via aerosol assisted chemical vapour deposition, *RSC Adv.* 6 (2016)
26. S.H. Santagneli, C.C. de Araujo, W. Strojek, H. Eckert, G. Poirier, S.J.L. Ribeiro, Y. Messaddeq, *J. Phys. Chem. B* 111 (2007) 10109.
27. L. Koudelka, I. Rosslerová, J. Holubová, P. Mosner, L. Montagne, B. Revel, *J. Non-Cryst. Solids* 357 (2011) 2816.
28. S.H. Santagneli, J. Ren, M.T. Rinke, S.J.L. Ribeiro, Y. Messaddeq, H. Eckert, *J. Non-Cryst. Solids* 358–6 (2012) 985–992.
29. C.Y. Wang, Z.X. Shen, B.V.R. Chowdari, *J. Raman Spectrosc.* 29 (1998) 819.
30. I. Shaltout, Y.I. Tang, R. Braunstein, A.M. Abu-Elazm, *J. Phys. Chem. Solids* 56 (1995) 141.
31. V.O. Sokolov, V.G. Plotnichenko, V.V. Koltashev, E.M. Dianov, *J. Non-Cryst. Solids* 352 (2006) 5618
32. S. Khatir, J. Bolka, B. Capoen, S. Turrel, M. Bouazaoui, *J. Mol. Struct.* 563–564 (2001) 283.
33. D. Munoz-Martin, M.A. Villegas, J. Gonzalo, J.M. Fernandez-Navarro, *J. European Cer. Soc.* 29 (2009) 2903.
34. J.P. Vigouroux, G. Calvarin, E. Husson, *Solid State Chem.* 45 (1982) 343.
35. D. Lezal, J. Horak, J. Navratil, S. Karamazov, A. Sklenar, *Phys. Chem. Glasses* 42 (2001) 324.
36. M. Łukaszewicz, B. Klimesz, A. Szmalec et al., *Journal of Alloys and Compounds*, <https://doi.org/10.1016/j.jallcom.2020.157923>
37. R.T. Karunakaran, K. Marimuthu, S. Arumugam, S. Surendra Babu, S.F. LeonLuis, C.K. Jayasankar, *Structural, Opt. Mater.* 32 (2010) 1035–1041.
38. T. Srikumar, M.G. Brik, Ch. Srinivasa Rao, Y. Gandhi, D. Krishna Rao, V. Ravi Kumar, N. Veeraiah, *Spectrochim. Acta Part A Mol. Biomol. Spectrosc.* 81 (2011) 498–503.
39. W.T. Carnall, H. Crosswhite, H.M. Crosswhite, Argonne National Laboratory, Argonne, USA, 1977.
40. W.T. Carnall, P.R. Fields, K. Rajnak, *J. Chem. Phys.* 49 (1968) 4412–4423.